JAERI-M
89-036

EXPERIMENTAL OBSERVATION OF ION BERNSTEIN WAVE HEATING ON JFT-2M TOKAMAK

March 1989

Hiroshi TAMAI, Toshihide OGAWA, Hiroshi MATSUMOTO and Kazuo ODAJIMA

日本原子力研究所
Japan Atomic Energy Research Institute

JAERI-M レポートは，日本原子力研究所が不定期に公刊している研究報告書です。
入手の問合わせは，日本原子力研究所技術情報部情報資料課（〒319—11 茨城県那珂郡東海村）あて，お申しこしください。なお，このほかに財団法人原子力弘済会資料センター（〒319-11 茨城県那珂郡東海村日本原子力研究所内）で複写による実費頒布をおこなっております。

JAERI-M reports are issued irregularly.
Inquiries about availability of the reports should be addressed to Information Division, Department of Technical Information, Japan Atomic Energy Research Institute, Tokai-mura, Naka-gun, Ibaraki-ken 319-11, Japan.

編集兼発行　日本原子力研究所
印　　刷　山田軽印刷所

JAERI-M 89-036

Experimental Observation of Ion Bernstein Wave Heating on JFT-2M Tokamak

Hiroshi TAMAI, Toshihide OGAWA
Hiroshi MATSUMOTO and Kazuo ODAJIMA

Department of Thermonuclear Fusion Research
Naka Fusion Research Establishment
Japan Atomic Energy Research Institute
Naka-machi, Naka-gun, Ibaraki-ken

(Received February 28, 1989)

Plasma heating by Ion Bernstein Wave (IBW) on JFT-2M tokamak is reported.

IBW is a kind of slow wave, therefore dominant coupling with plasma ions and efficient heating are expected. Since IBW launcher is located at low field side of torus, it is advantageous as a method to heat the future reactor plasma.

Our experiment is made at the generator frequency of $\omega=3/2\omega_H$ or $3\omega_D$, where ω_H, and ω_D are the ion cyclotron frequency of hydrogen and deuterium, respectively.

Plasma loading impedance increases as outermost plasma surface approaches to the IBW launcher, and in approaching case the impedance decreases as averaged electron density increases.

Increase of stored energy is observed by IBW heating. This is mainly contributed to density build-up, but a small part comes from net plasma heating. On the other hand, enhanced impurity radiation is observed during IBW heating, and the increment of radiation loss exceeds IBW launched power by a factor of two or three.

In order to reduce the radiation enhancement, optimum condition is searched by surveying several plasma parameters like as configuration, current, density, and concentration ratio of hydrogen in deuterium. However, maximum IBW launched power is only 150 kW.

Maximum launched power is increased up to 300 kW through the combination with neutral beam heating which compensates the radiation cooling.

As same as IBW only case, the radiation increment limits the maximum value of launched power. Enhancement of high energy hydrogen up to 10 keV is observed.

Loading impedance with H-mode plasma falls to about 40% of that with L-mode plasma, mainly due to the drastic change of edge plasma feature. H-mode plasma is terminated by only 20 kW of IBW power, because of edge plasma heating.

Keywords: Ion Bernstein Wave, JFT-2M Tokamak, Plasma Heating, Out-Side Launcher, Loading Impedance, Stored Energy, Radiation Cooling, H-mode Plasma

JAERI－M 89－036

JFT－2Mトカマクにおけるイオンバーンシュタイン波加熱

日本原子力研究所那珂研究所核融合研究部
玉井　広史・小川　俊英・松本　宏・小田島　和男

（1989年2月28日受理）

JFT－2Mトカマクにおいて，イオンバーンシュタイン波によるプラズマ加熱実験を行った。イオンバーンシュタイン波は遅波の一種で，主にイオンと結合し，これを効率良く加熱することが知られている。また，波の励起の性質上，弱磁場側すなわちトカマク装置の外側から入射することができるので，将来の実験炉のプラズマを加熱する手段としても有効と考えられる。

実験は，$\omega = 3/2\,\omega_H$，及び$3\,\omega_D$（ω_H，ω_Dはそれぞれ水素と重水素のイオンサイクロトロン角周波数）の加熱モードで行った。

IBWのプラズマ負荷抵抗は，最外殻のプラズマがランチャーに近づくにつれて増加し，また，ある程度近づいた状態では電子密度の増加に伴って減少した。

IBW加熱時に蓄積エネルギーの増加が観測された。これは主としてIBW加熱中の密度上昇が起因しているが，わずかではあるがプラズマの加熱も寄与していた。一方，IBW加熱中に輻射損失の顕著な増加が観測され，この増加量はIBW入力パワーの2－3倍に達した。

輻射損失を出来るだけ抑えるために，プラズマの配位，プラズマ電流，水素／重水素の混合比などをパラメータとして最適条件を探したが，最大150 kWのパワー入力しか得られなかった。

輻射損失による冷却を補償するために中性粒子ビーム（NBI）との組み合せ加熱をした結果，パワー入力を300 kWまで増加させることができた。しかしながら，パワーの上限はIBW単独のときと同様に輻射損失の増大で決まっていた。このとき，水素のエネルギースペクトルで2－10 keVの領域が増加していた。

Hモードでのプラズマ負荷抵抗はLモードの40％に減少したが，これは，ランチャー近傍のプラズマの状態が大きく変化したためと考えられる。また，Hモードプラズマは，わずか20 kWのIBW入力パワーでもLモードに遷移した。このとき，スクレイプオフ層の電子温度の上昇が観測され，Lモードへの遷移はこのスクレイプオフ層のプラズマの加熱が起因していると考えられる。

那珂研究所：〒311－01　茨城県那珂郡那珂町大字向山801－1

Contents

目　　次

1. INTRODUCTION

Plasma heating by Ion Cyclotron Range of Frequency(ICRF) is one of the attractive method because of locality of heating position, and high power accessibility. On JFT-2M, heating through the higher-field-side launcher has been done in advantage of high coupling and absorbing efficiency through mode conversion. Successive results like impurity control[1], transition to H-mode[2] have been observed.

In considering the wave heating in future reactor scale plasma, the low field side launcher is suitable for the operation and maintenance. However, plasma intends to leave away from the antenna especially in H-mode discharge, then the wave coupling of plasma in conventional out-side launcher becomes less with the decease of plasma density. In contrast to these out-side launcher, the Ion Bernstein Wave(IBW) heating is estimated not to degradate the plasma coupling.[3]

It is necessary to clarify the plasma response like coupling, and power absorption by IBW heating in H-mode phase. On this view point IBW heating experiment is done on JFT-2M. In our experiment, IBW does not achieve efficient plasma heating due to induction of extremely enhanced radiation loss. IBW does not launched efficient power for H-mode transition, in addition, a small launched power into H-mode plasma forces L-mode transition. Then, the coupling efficiency with several plasma configurations are investigated at relatively lower IBW power.

This report presents the experimental observation during IBW heating, several attempts to increase the launched power to plasma, and investigation of coupling characteristics with H-mode plasma..

2. EXPERIMENTAL SETUP

2.1 Heating Regime

Heating regime of 3/2 harmonic ion cyclotron resonance of hydrogen or third harmonic resonance of deuterium is selected, since Ion Bernstein Wave is well absorbed in that resonance layer.[4][5] The harmonic resonance layers existed in JFT-2M torus at the generator frequency of 27MHz are shown in Fig.1. The resonance layer of 3/2 harmonic of hydrogen or third of deuterium allocates at the center of magnetic axis when toroidal magnetic field strength(B_T) is 1.18T.

2.2 Launcher Configuration

The IBW launcher used in our machine is B_θ - E_z type loop antenna which makes the RF current in the toroidal direction,[4] as shown in Fig.2(a). Launcher is constructed by inner conductor made of cooper metalled stainless steel, two layers of Faraday shield made of titanium, and side protector of carbon graphite. As shown in Fig.2(b)(c), the launcher is installed at oblique port on JFT-2M, with angle of 43° to the horizontal plane.

3. RESULTS AND DISCUSSION

3.1 Loading Impedance

At first, plasma loading impedance is investigated for plasma configurations of D-shaped limiter and upper single null divertor. Dependence on the averaged electron density is shown in Fig.3. In D-shaped limiter configuration, the loading impedance goes down as density goes up. On the other hand, in upper single null divertor configuration there seems to be no strong dependence on averaged density. In addition, loading impedance is much different in different configuration even at the same averaged density. The dominant difference between these configurations is the distance between IBW launcher and the plasma (ΔR). Then, the loading impedance is replotted versus the distance ΔR, which is deduced from outermost magnetic surface. Figure 4 shows this dependence for density region of $2.0\text{-}3.5\times10^{19}m^{-3}$. It is obvious that the loading impedance becomes larger as plasma approaches to the launcher. It is considered that in the D-shaped limiter plasma approaches very close to the launcher and the surrounding plasma is influenced by the feature of main plasma region; on the other hand in single null divertor, the influence of main plasma region is not so much because of sufficient isolation between outermost plasma and launcher. These results show that the loading impedance is very sensitive to edge plasma around the launcher and qualitatively agrees well with the theoretical estimation.[3]

3.2 Optimization of Resonance Layer

An optimum absorption and heating position of IBW is searched by surveying the strength of toroidal magnetic field. The survey range from 1.0T to 1.34T includes the resonance layer of $\omega_H(2\omega_D)$, $3/2\omega_H(3\omega_D)$ and $2\omega_H(4\omega_D)$, where ω_H and ω_D are the ion cyclotron frequency of hydrogen and deuterium.

B_T-survey is done in the following plasma parameters; plasma species of a few percent of hydrogen mixture in deuterium, configuration of upper single null divertor, plasma current of 240kA, density of 2.3×10^{19} m^{-3} before IBW power input(OH phase). IBW power of about 120kW is coupled with plasma.

The heating efficiency is investigated by the increments of plasma stored energy W_s obtained by diamagnetic measurement, and by the increments of electron density and radiation loss power P_r. Figure 5 shows these increments dependence on toroidal magnetic field strength.

The increments are larger around B_T=1.2T. From this figure the dependence of power absorption on toroidal magnetic field may be expected. This possibility is checked by the estimation of IBW absorbed power in plasma from the decay of stored energy after IBW turns off.[1] Figure 6 shows the absorption efficiency which is determined by absorbed power divided by launched power. Dependence on B_T is week in contrast with that of stored energy or radiation loss increment. Therefore, plasma heating efficiency is better when the $3/2\omega_H$ or $3\omega_D$ resonance layer locates around the plasma center; that is B_T=1.18T.

3.3 Feature of Plasma Parameters

Figure 7 shows the temporal variation of typical plasma parameters with IBW of about 120kW at B_T of 1.18T in upper single null divertor. As clearly seen, after initiation of IBW pulse the density and radiation loss increase, and in similar manner, loop voltage goes up. Electron temperature measured by Electron Cyclotron Emission(ECE) decreases, but stored energy increases slightly. These behaviors show the increase of impurity contamination. In this case, increments of the radiation loss reaches as three times as IBW launched power. The negative margin is supported by the ohmic heating power. The ratio of total radiation loss to total input power increases from 40% at OH-phase to about 90% during IBW-phase.

Typical impurity line emission is shown in Fig.8. Impurity lines are carbon which is the material of limiter and wall panel, titanium of antenna Faraday shield and sublimation layer, iron of the wall base, and oxygen. These impurity lines are all enhanced about factor of two or three during IBW pulse. Especially titanium and iron intensities rapidly rise at the onset of IBW.

The radiation profile is observed by horizontal bolometer array.[6] Viewing area of each chord is shown in Fig.9(a). Figure 9(b) shows an intensity of each viewing chord(before Abel inversion) of the same shot in Fig.7. During IBW pulse, the radiation in the central chords largely increase than the peripheral chords; this indicates the accumulation of impurity in the plasma center region.

From these observation, it is confirmed that IBW enhances the impurity influx especially metal impurity influx, and enhanced radiation induces the

plasma cooling down.

Stored energy is plotted versus electron density in the case of upper single null divertor. Figure 10 compares that during IBW phase [+] and that ohmic phase [○]. Stored energy during IBW is slightly larger than that of OH phase. Thus, the increase of stored energy by IBW is mainly due to the density build-up, but a small fraction of stored energy increase is contributed by net heating by IBW. In this case about 1kJ of heating is observed by 120kW IBW power. Global energy confinement time(τ_E) is reduced from 40ms at OH-phase to 20ms at IBW-phase. This value is less by a factor of two or more than that in conventional mode conversion heating by high field side launcher on JFT-2M tokamak.[2][7]

3.4 Attempt for more power launching

In order to reduce the radiation enhancement and maintain the plasma heating by IBW, we search the optimum condition by surveying several plasma parameters. Surveyed parameters are configuration, current, and concentration ratio of hydrogen in deuterium.

3.4.1 Plasma Configuration and Concentration Ratio

Figures 11 shows the radiation increments versus IBW launched power in the configuration of circular, upper or lower single null divertor, and D-shaped limiter discharge. Concentration of hydrogen is about half ratio (a), a few percent(b) and almost pure hydrogen(c). Among these concentration ratio, radiation increments are the minimum at half ratio case, although increments also exceeds the launched power. The maximum launched power is about 150kW. Little differences are observed between the different configurations.

The radiation increments versus launched power in the case of mode conversion heating is plotted in Fig.12. In this case, plasma configuration is upper or lower single null divertor, plasma current is 200kA, toroidal magnetic field is 1.2T, RF generator frequency is 16.8MHz, and concentration ratio of hydrogen is nearly 40% in deuterium. Radiation increments never exceeds the launched power, and launched power more than 600kW is attainable. In contrast to mode conversion heating, our IBW heating gives an extremely large impurity radiation.

In Fig.13, stored energy versus density is compared between two cases of hydrogen concentration of half ratio(○) and a few percent(+). Stored energy in the half ratio case is slightly larger than that in a few percent case; that is considered to be from less radiation enhancement.

3.4.2 Plasma Current

The next parameter is plasma current as shown in Fig.14. At three type of plasma current of 100kA, 200kA, and 270kA, increments of radiation loss versus IBW power is plotted. Higher IBW power input is available in higher plasma current because of the stronger support of ohmic input power. However the radiation loss exceeds the IBW power by a factor of about 1.5.

3.5 Combination with NBI

In order to compensate the cooling by enhanced radiation and to couple more IBW power, the combination heating with neutral beam injection is examined.

Hydrogen neutral beam of 570kW is injected into deuterium plasma with pulse length of 300ms. IBW power of 300kW with pulse length of 200ms starts at 100ms after the initiation of NBI.

Temporal variation of typical plasma parameters are shown in Fig.15. Increments of stored energy, radiation, and density versus B_T are plotted in Fig.16. In this case good heating is investigated in narrow region around B_T=1.3T. At B_T=1.1T, radiation is large, however stored energy decreases. This means cooling rather than heating by IBW.

Radiation Increment versus IBW launched power is plotted in Fig.17. As similar to IBW only case, radiation increments exceeds the launched power by a factor of 1.5. However maximum launched power increases to about 300kW by compensating of radiation loss power with NBI power.

Hydrogen and deuterium ion energy spectra are observed by charge exchange measurement(CX) in perpendicular direction. Figure 18 shows the comparison of energy spectrum during NBI phase and during NBI with IBW phase. Hydrogen energy up to 10keV is enhanced, and this corresponds to perpendicular ion temperature increase from 0.7keV at NBI phase to about 1keV. On the contrary,

deuterium ion temperature does not change. At present, it is not distinguish that the increase of energetic hydrogen is caused whether by central ion heating or by peripheral neutral enhancement.

3.6 Launching to H-mode plasma

IBW power is launched to H-mode plasma produced by NBI in single null divertor. Temporal variation of density, H_α/D_α emission, radiation loss, and stored energy are shown in Fig.19. In this shot, IBW launched power is about 100kW. H-mode transition occurs at 610ms with sudden depletion of H_α/D_α emission, consequently density, and stored energy increase. At the onset of IBW pulse at 700ms, H-mode is terminated with sudden jump-up of H_α/D_α emission. The termination of H-mode is observed above 20kW of IBW launched power.

Electrostatic probe measurements show the behavior of scrape-off plasma. As shown in Fig.20, sudden increase of electron temperature in scrape-off plasma T_e^{so} is observed at the onset of IBW pulse, which is in contrast to lower constant value at H-mode phase. Two mechanisms for H- to L-mode transition might be considered when some fraction of IBW power is absorbed in the edge plasma. One is that the increase of edge electron temperature enhances the sputtering yield, and through the increase of impurity influx H-mode would be terminated. The other is that the edge plasma heating would destroy the temperature pedestal at the plasma edge which is required to keep the H-mode plasma.[8][9] It is not yet distinguished which mechanism is dominant to H- to L-Transition by IBW input.

By launching IBW with lower power than 20kW, the change of loading impedance with H-mode plasma is observed. Figure 21 shows the behavior of loading impedance in the upper single null divertor. At the instant of H-mode transition, loading impedance falls rapidly to 0.25Ω from 0.65 Ω at L-phase. at the transition from L-phase to H-phase average density increases from 2×10^{19} m^{-3} to $4\times10^{19}m^{-3}$, whereas the distance between outermost plasma and launcher changes not so much from 9.2cm to 9.6cm. It should be remembered that the loading impedance is independent on the averaged density but gradually decrease with increasing distance between plasma and the launcher in the upper single null divertor as shown in Fig.3. Therefore, change of another plasma feature is necessary for relating to the rapid drop of loading impedance with H-mode plasma. It is observed that in H-mode phase density in scrape-off layer quickly decreases, and increases at the H- to L- transition as shown in Fig.20; it changes in similar

manner to that of the loading impedance. Thus the decreases of loading impedance during H-mode phase is considered to be mainly due to the drop of scrape-off density, and this fact qualitatively agrees well again with the theoretical estimation.[3]

4. SUMMARY

Ion Bernstein Wave(IBW) is launched to several parameters of plasma on JFT-2M tokamak. Better coupling and heating is observed when $3/2\,\omega_H$ and $3\,\omega_D$ resonance layer is allocated on the plasma center.

Plasma loading impedance increases as outermost plasma surface approaches to the IBW launcher, and in approaching case the impedance decreases as averaged electron density increases. Loading impedance is seemed to have a strong dependence on edge plasma feature.

Increment of stored energy during IBW is mainly contributed from the density build-up, and a small part of store energy rise is due to the net plasma heating.

Enhanced radiation loss is observed and its increment exceeds the launched IBW power by a factor of two or more. Because of the radiation limit, IBW launched power of 150kW is the maximum value. Although various parameters such as plasma configuration, hydrogen concentration ratio, and plasma current, are surveyed in order to suppress the radiation enhancement, good heating aspect is not observed.

Even combination heating with neutral beam injection, enhanced radiation of 1.5 times as launched power is observed and the radiation loss limits the maximum launched power at 300kW. Hydrogen energy up to 10keV is enhanced by IBW.

Launching to the H-mode plasma shows a rapid transition to L-mode by launched power above 20kW. This is considered to be induced by heating of edge plasma.

Loading impedance with H-mode plasma is less than that with L-mode plasma mainly due to decrease of scrape-off density.

ACKNOWLEDGEMENT

The authors are grateful to the members of the JFT-2M experiment group for their constructive advice and fruitful discussion. They also thank the members of JFT-2M operation group for their excellent co-operation and helpful support.

They are indebted to Drs. H. Maeda, S. Shimamoto, M. Tanaka, and M. Yoshikawa, for their continuous encouragement.

REFERENCES

[1] H. Tamai, et al., Nuclear Fusion 26 (1986) 365.
[2] H. Matsumoto, et al., Nuclear Fusion 27 (1987) 1181.
[3] M. Brambilla, Nuclear Fusion 28 (1988) 549.
[4] M. Ono, et al., in Proc. of 11th Int. Conf. on Plasma Phys. and Cont. Nucl. Fusion Research (Kyoto, Nov. 1986) IAEA-CN-47/F-I-3) I-pp.477.
[5] Y. Ogawa et al., Nuclear Fusion 27 (1987) 1379.
[6] H. Tamai, et al., JAERI-M 88-120 (1988).
[7] K. Odajima, et al., JAERI-M 86-033 (1986).
[8] K. Hoshino, et al., Physics Letters A 124 (1987) 299.
[9] T. Yamauchi and JFT-2M Group, Jpn. J. Appl. Phys. 27 (1988) 924.

ACKNOWLEDGEMENT

The authors are grateful to the members of the JFT-2M experiment group for their constructive advice and fruitful discussion. They also thank the members of JFT-2M operation group for their excellent co-operation and helpful support.

They are indebted to Drs. H. Maeda, S. Shimamoto, M. Tanaka, and M. Yoshikawa, for their continuous encouragement.

REFERENCES

[1] H. Tamai, et al., Nuclear Fusion 26 (1986) 365.
[2] H. Matsumoto, et al., Nuclear Fusion 27 (1987) 1181.
[3] M. Brambilla, Nuclear Fusion 28 (1988) 549.
[4] M. Ono, et al., in Proc. of 11th Int. Conf. on Plasma Phys. and Cont. Nucl. Fusion Research (Kyoto, Nov. 1986) IAEA-CN-47/F-I-3) I-pp.477.
[5] Y. Ogawa et al., Nuclear Fusion 27 (1987) 1379.
[6] H. Tamai, et al., JAERI-M 88-120 (1988).
[7] K. Odajima, et al., JAERI-M 86-033 (1986).
[8] K. Hoshino, et al., Physics Letters A 124 (1987) 299.
[9] T. Yamauchi and JFT-2M Group, Jpn. J. Appl. Phys. 27 (1988) 924.

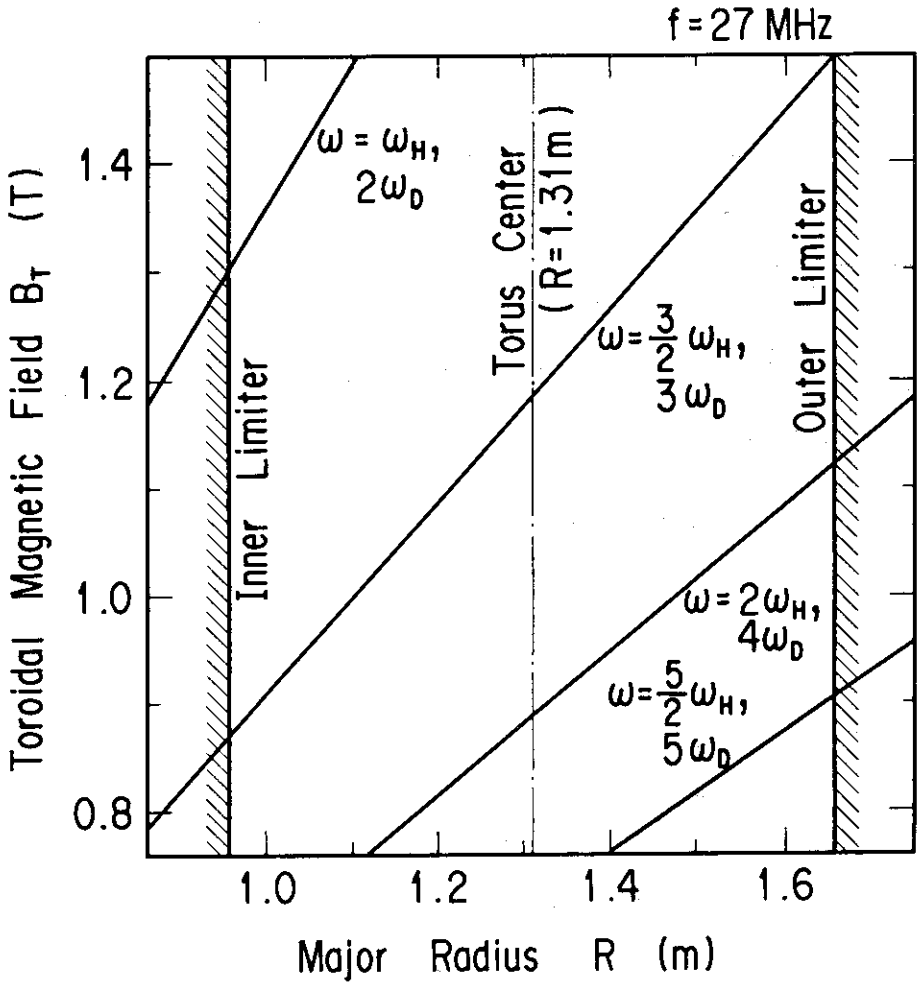

Fig.1 Harmonic resonance layer in JFT-2M torus.

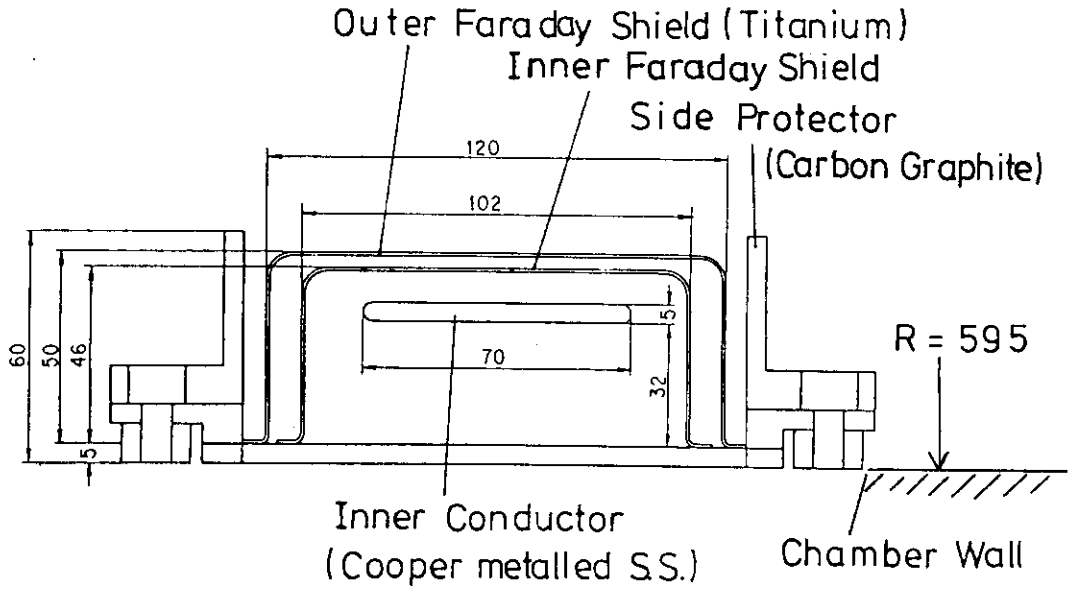

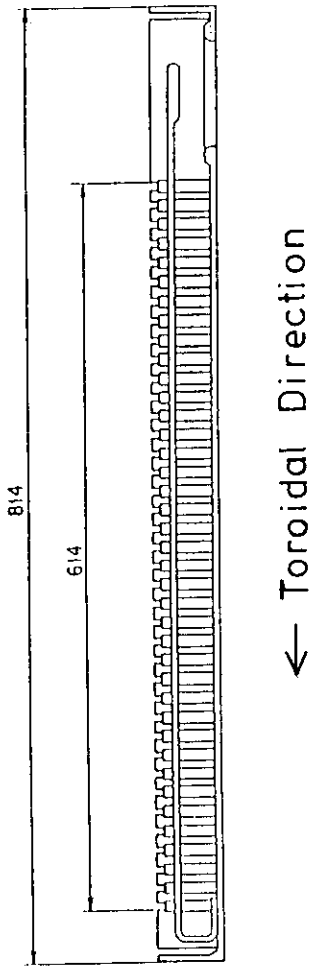

(a)

Fig.2 (a) Structure of IBW launcher.

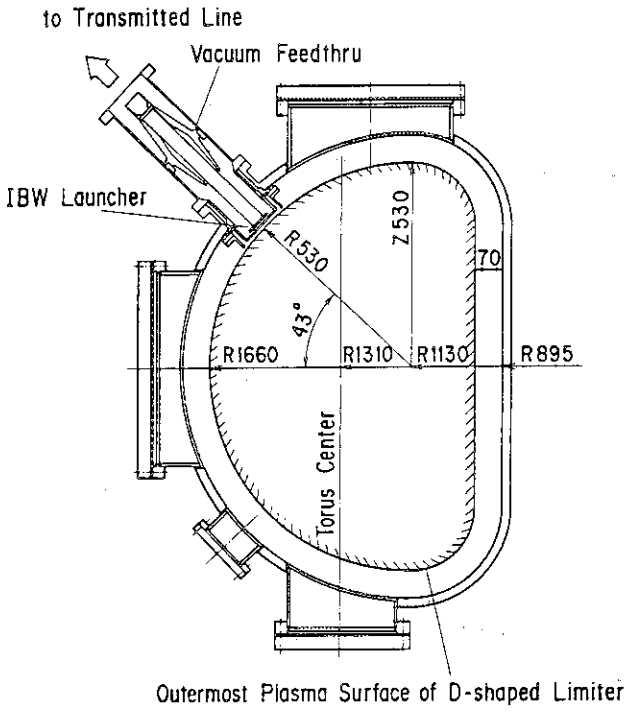

(b)

Fig.2 (b) Installation of IBW launcher on the torus (poloidal cross section).

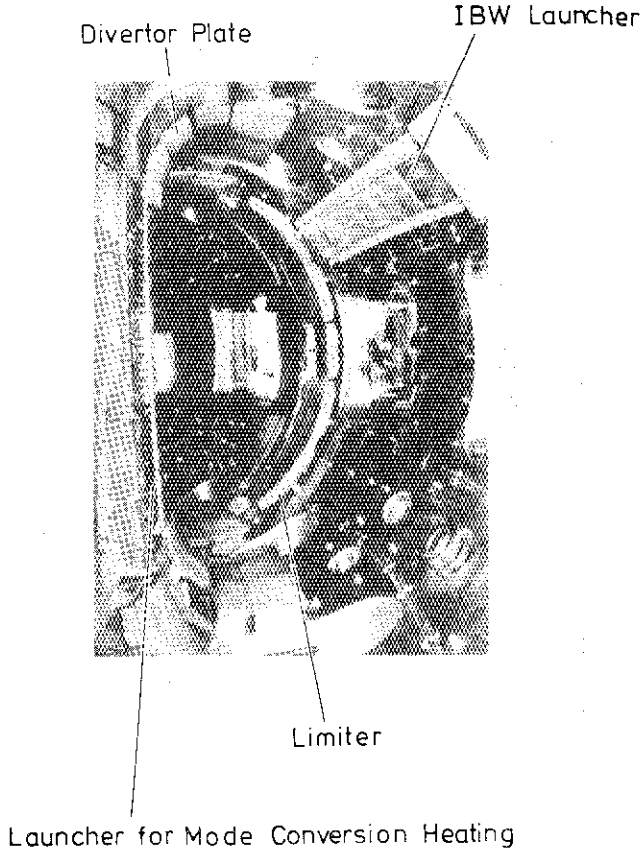

(c)

Fig.2 (c) Installation of IBW launcher (tangential viewing chord).

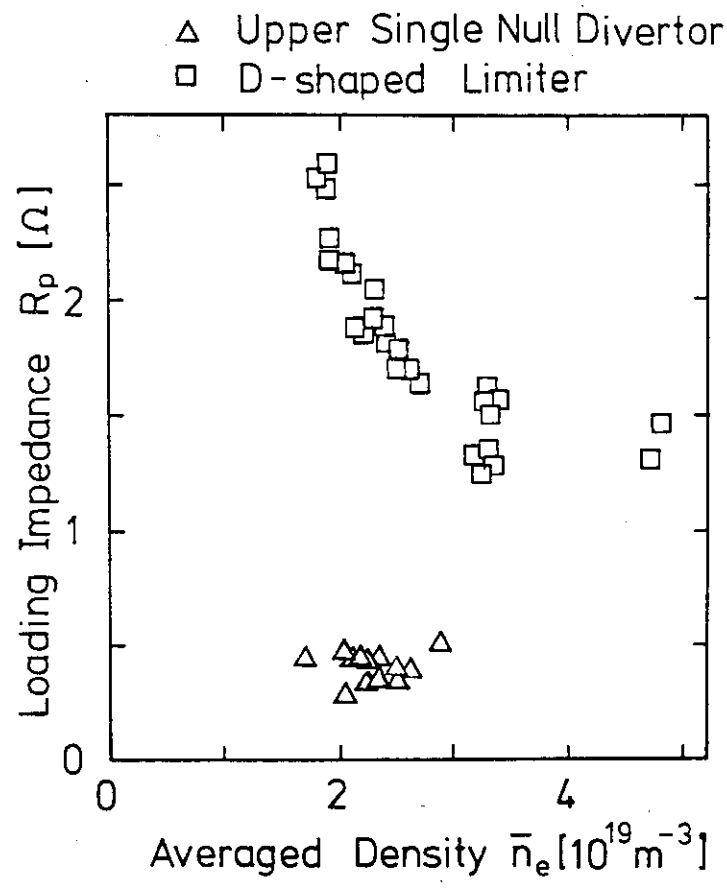

Fig.3 Dependence of plasma loading impedance on averaged electron density.

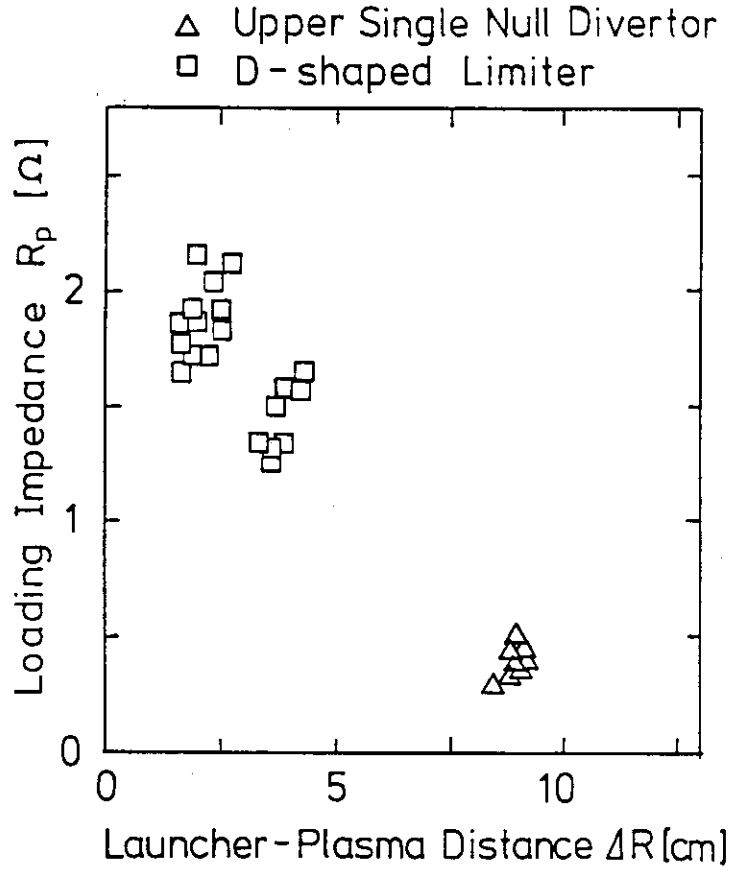

Fig.4 Dependence of plasma loading impedance on distance between launcher and outermost plasma.

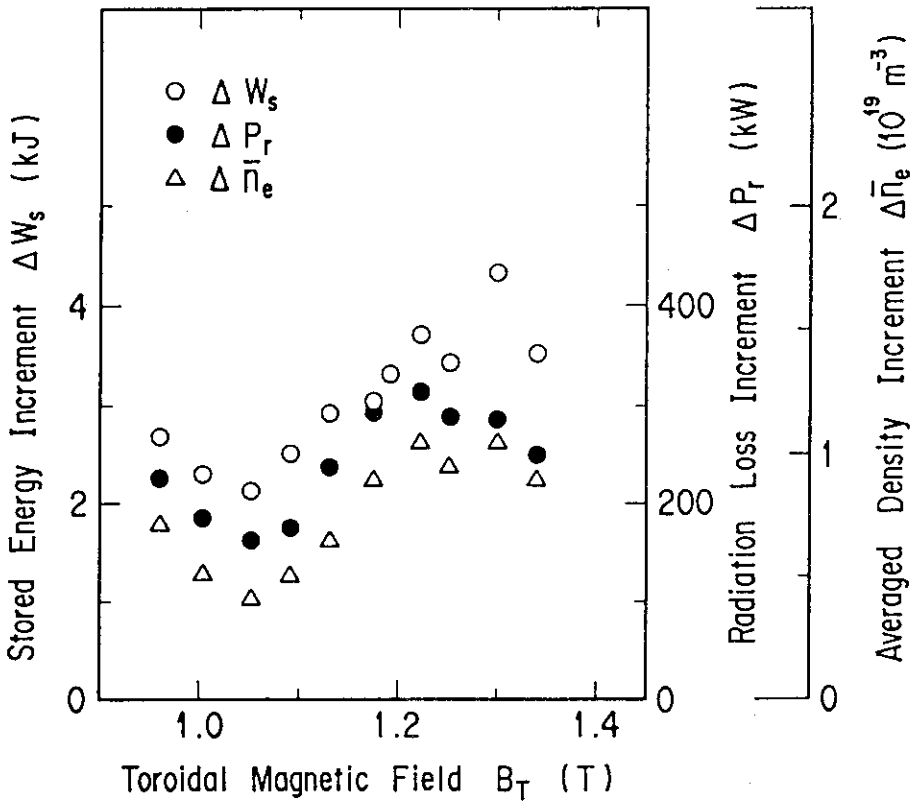

Fig.5 Increments dependence of stored energy(○), radiation loss(●), and density(△) on toroidal magnetic field strength.

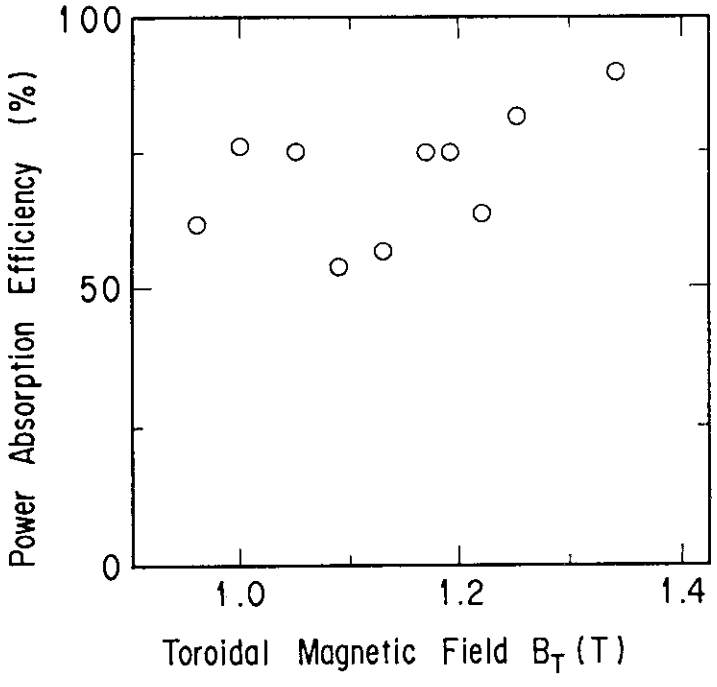

Fig.6 Absorption efficiency of IBW power.

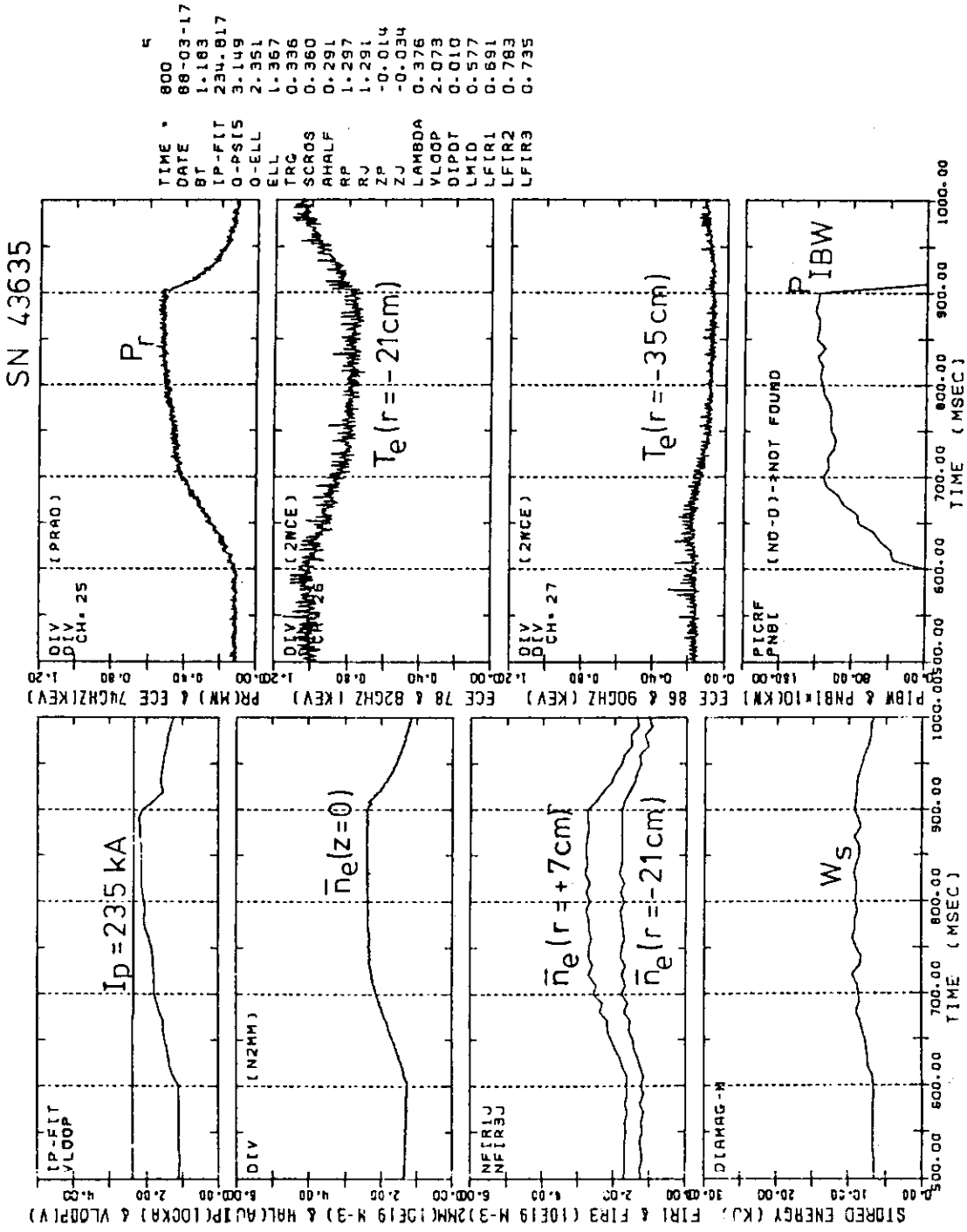

Fig.7 temporal variation of typical plasma parameters with IBW heating in upper single null divertor.

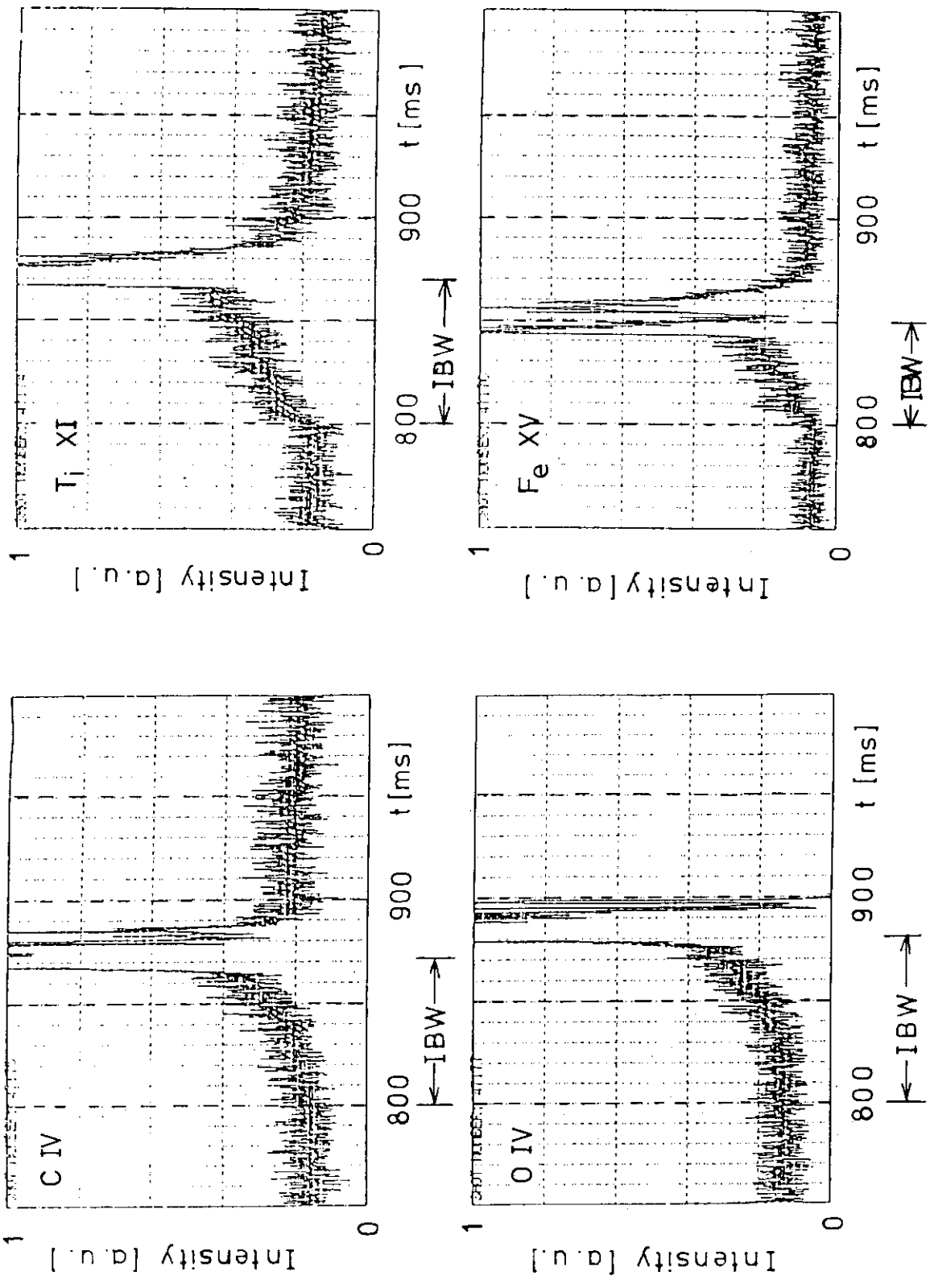

Fig.8 Typical impurity line emission.

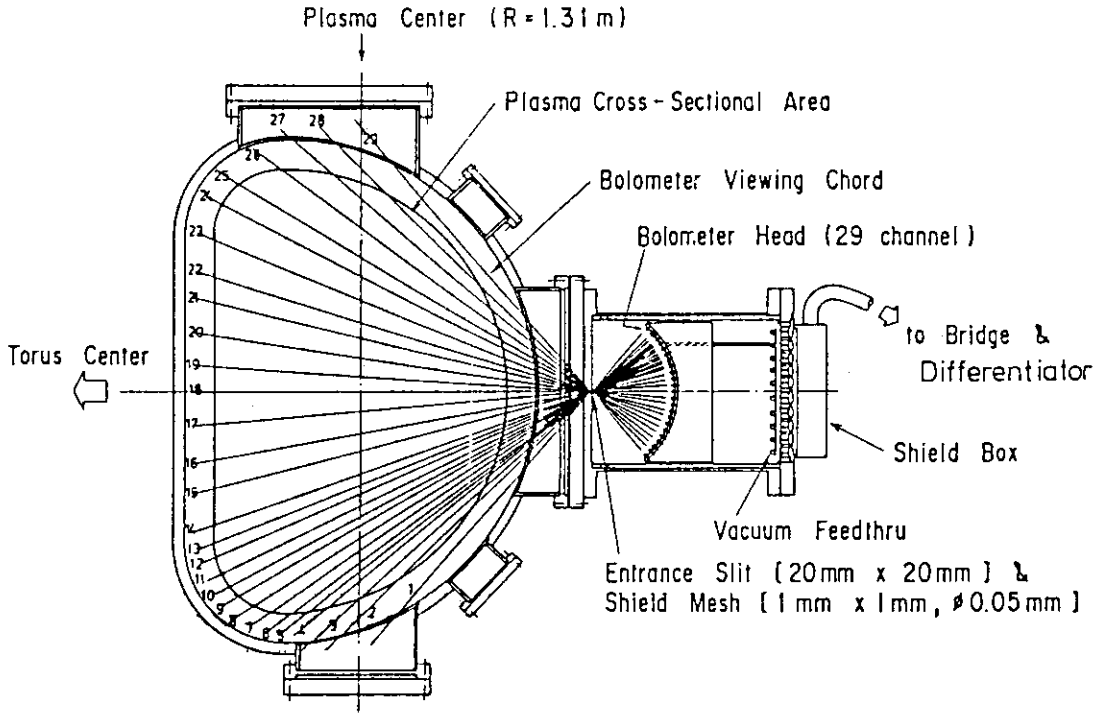

Fig.9 (a) Viewing chord of horizontal bolometer array.

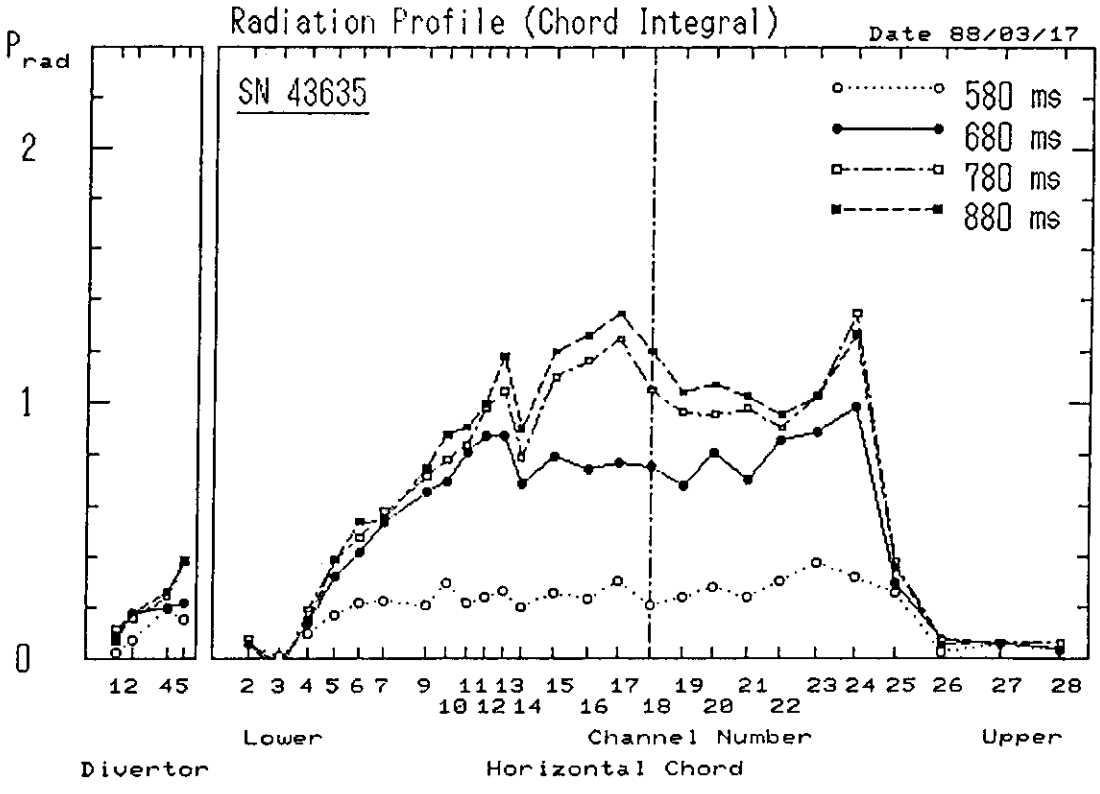

Fig.9 (b) Chord integrated radiation profile (before Abel inversion).

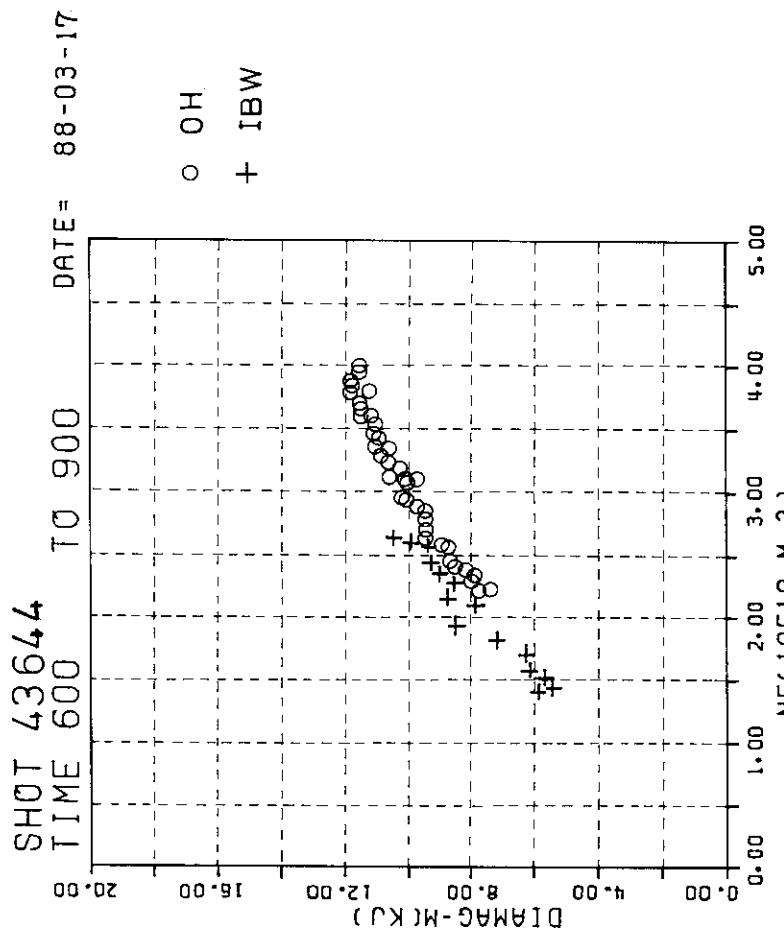

Fig.10 Comparison of stored energy on density dependence between OH (○) and IBW (+).

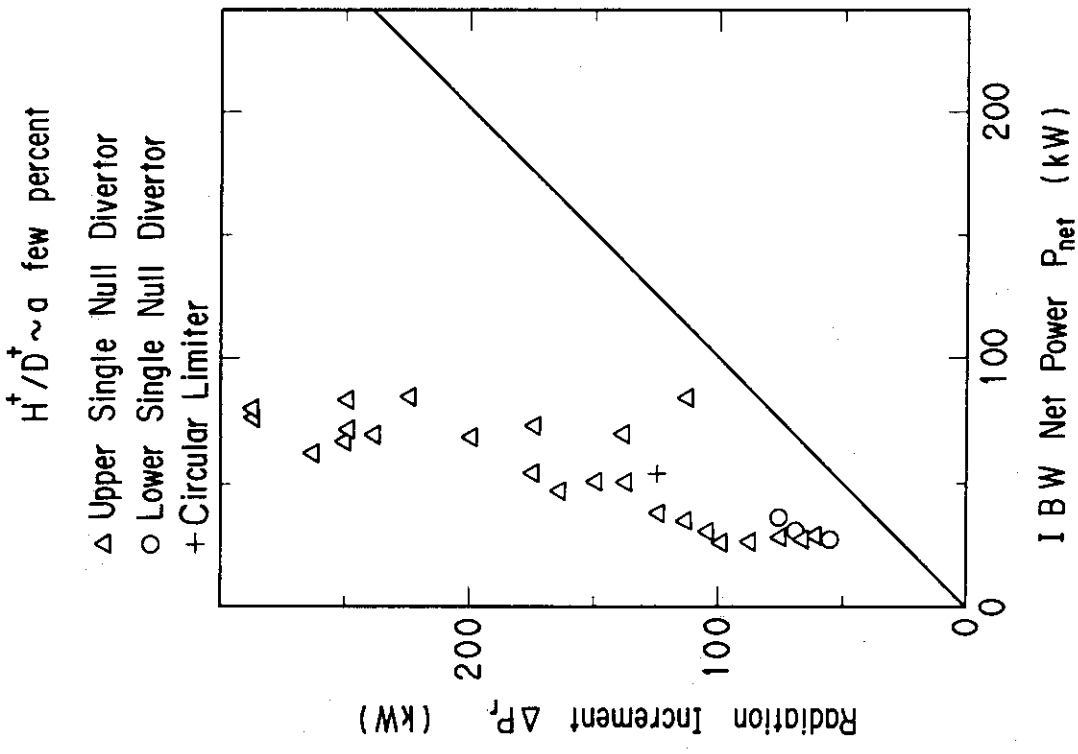

Fig.11 (b) that of a few percent.

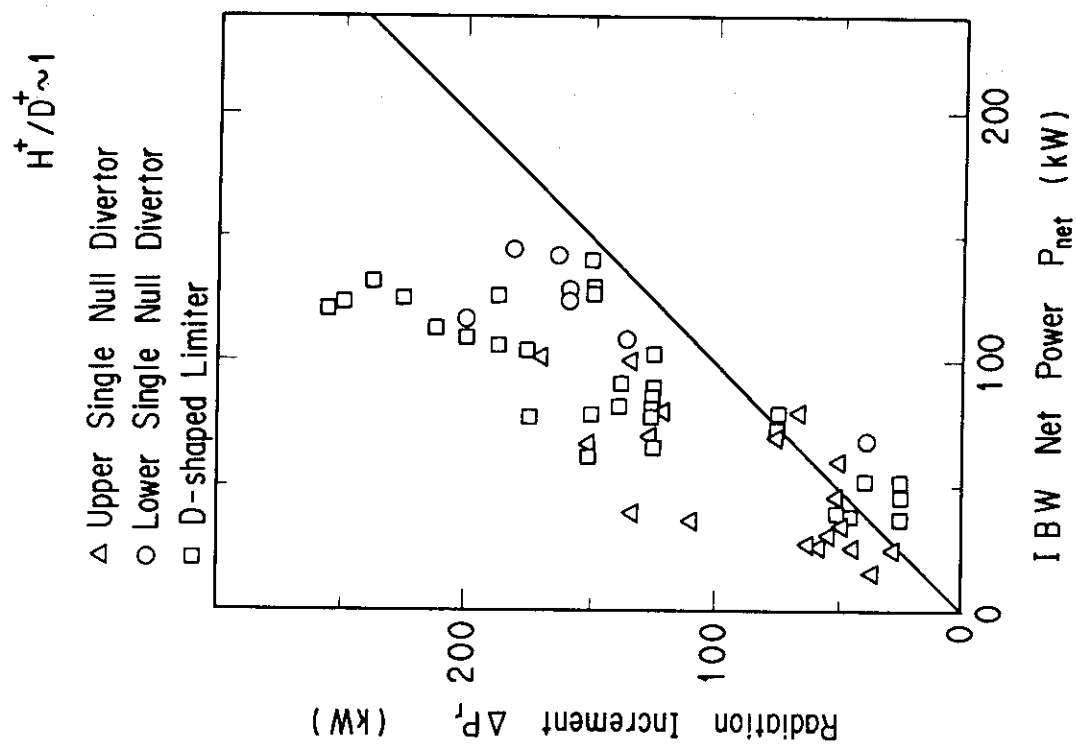

Fig.11 (a) Radiation increments in hydrogen concentration of half.

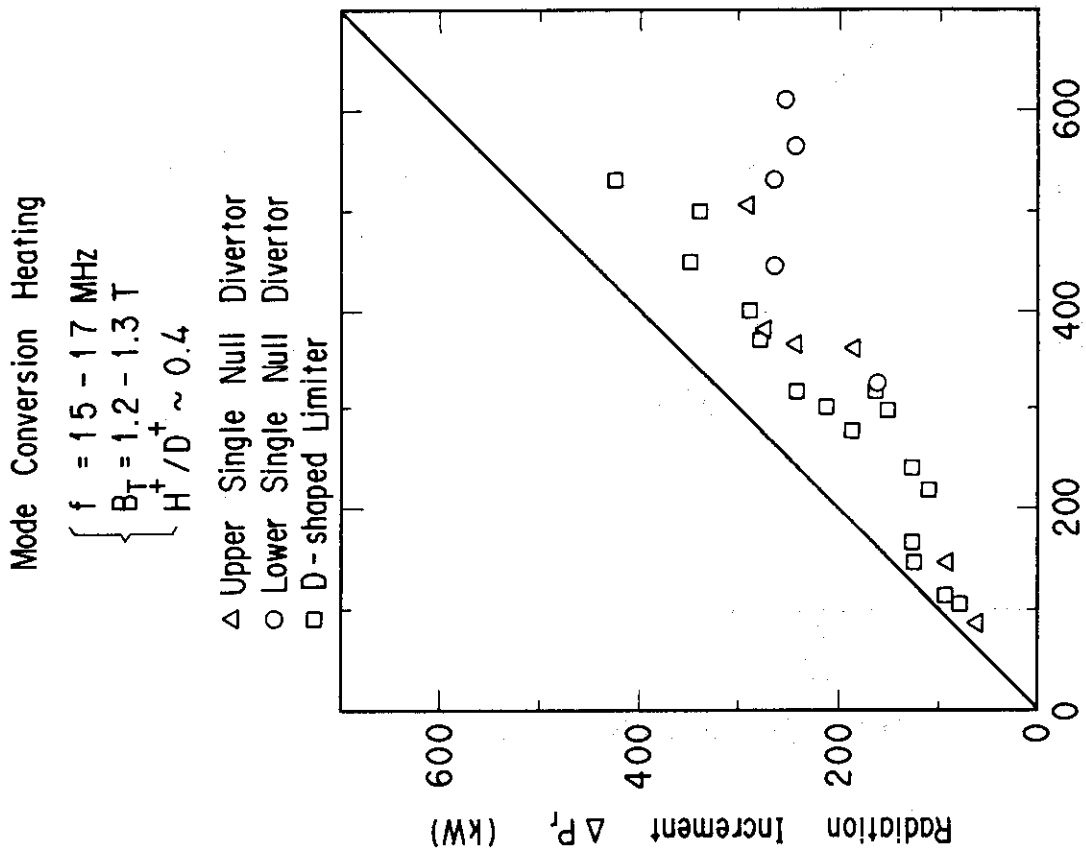

Fig.12 Radiation increments in mode conversion heating.

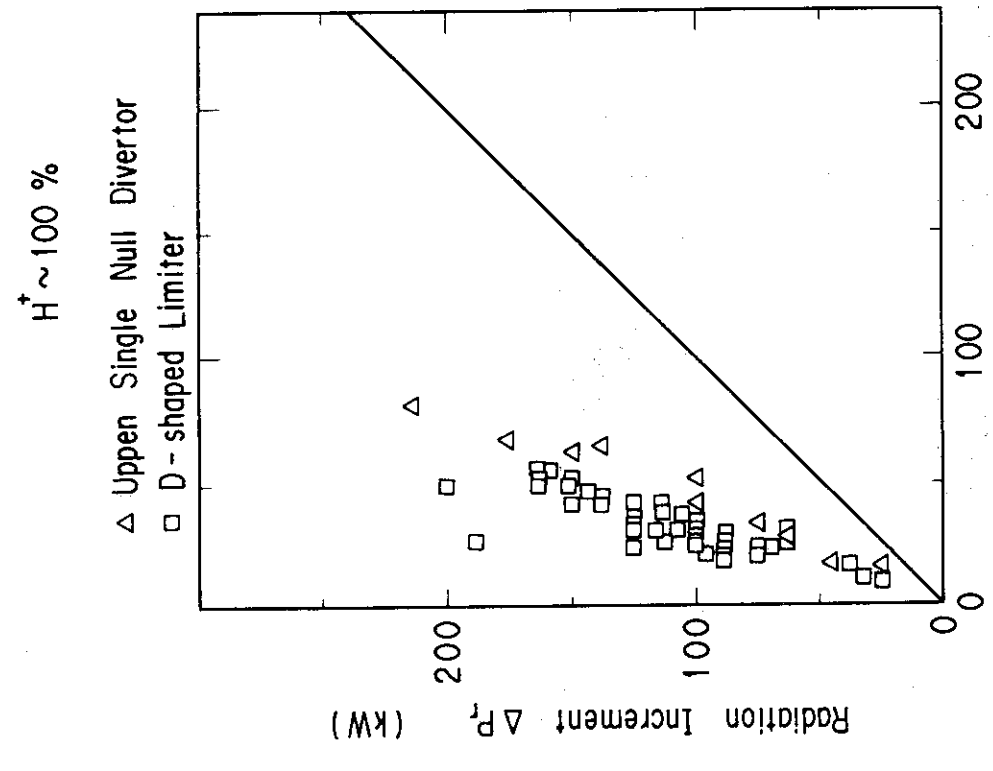

Fig.11 (c) that of almost pure hydrogen.

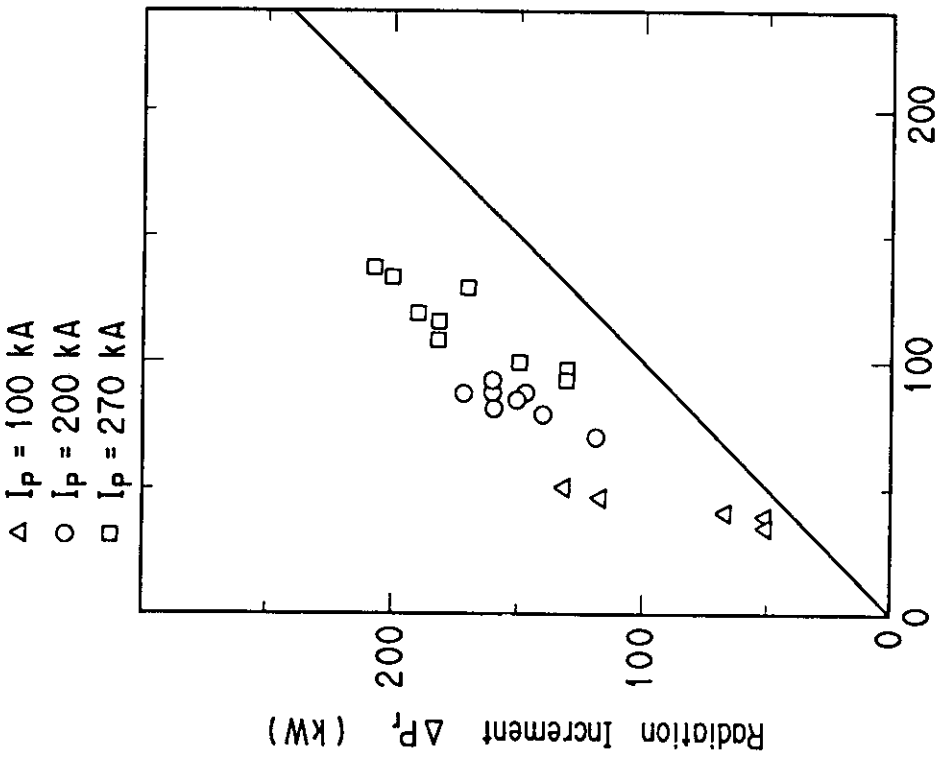

Fig.14 Radiation increments at the survey of plasma current.

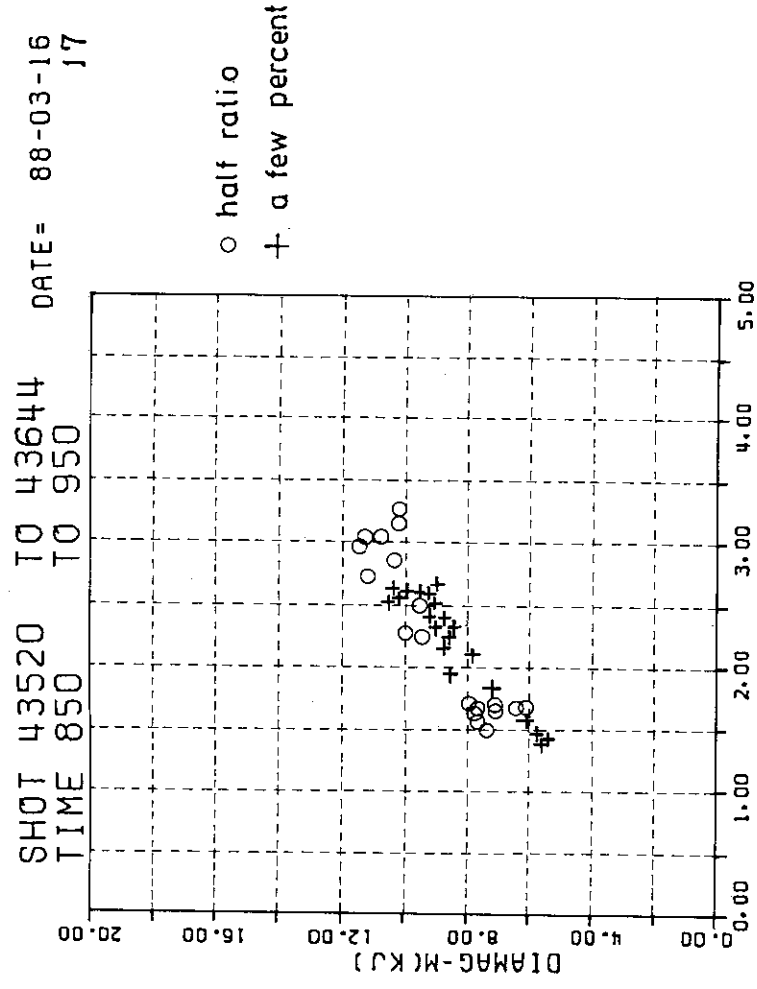

Fig.13 Comparison of stored energy on density dependence between two cases of hydrogen concentration of half ratio(○) and a few percent(+).

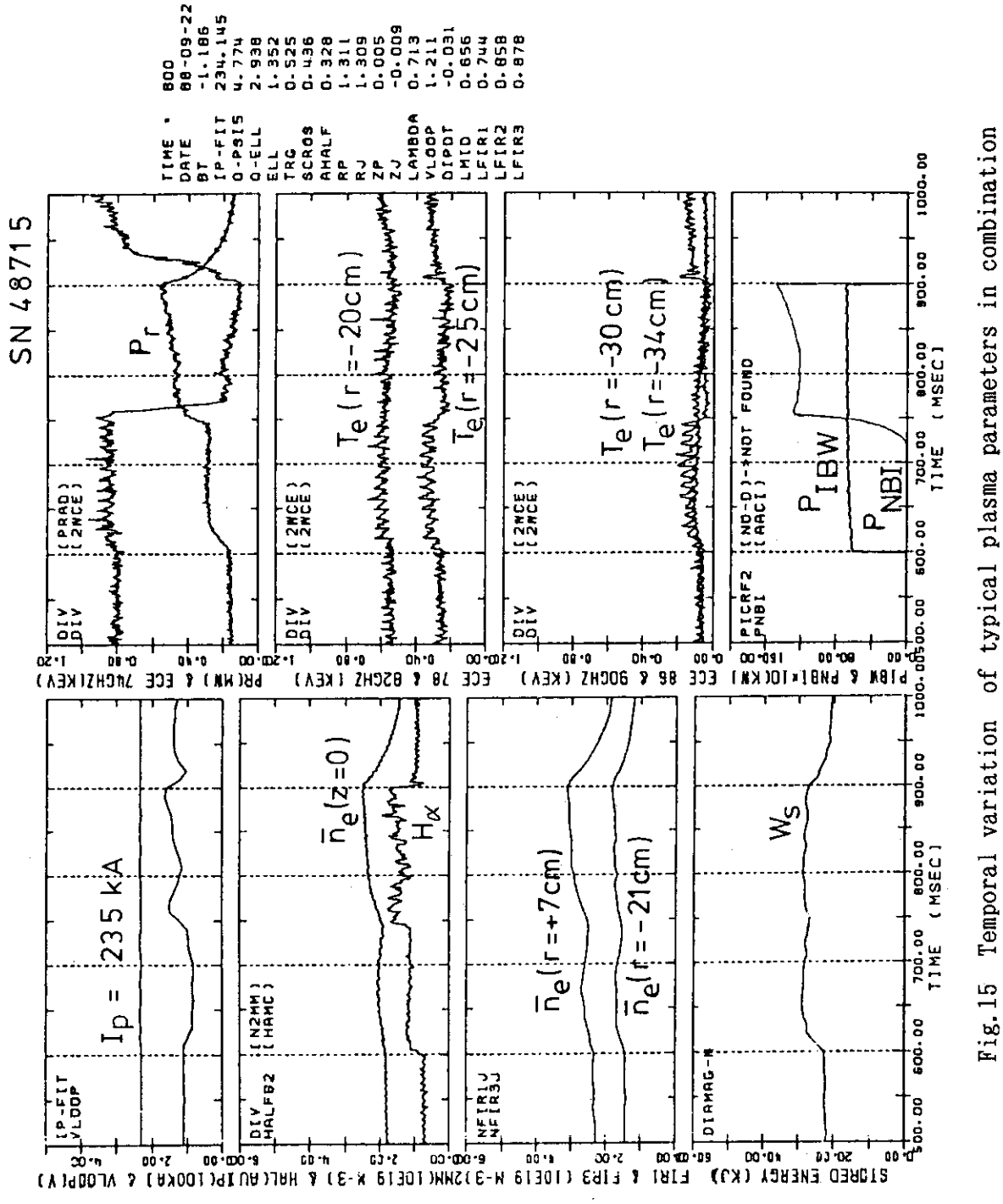

Fig.15 Temporal variation of typical plasma parameters in combination heating of NBI and IBW.

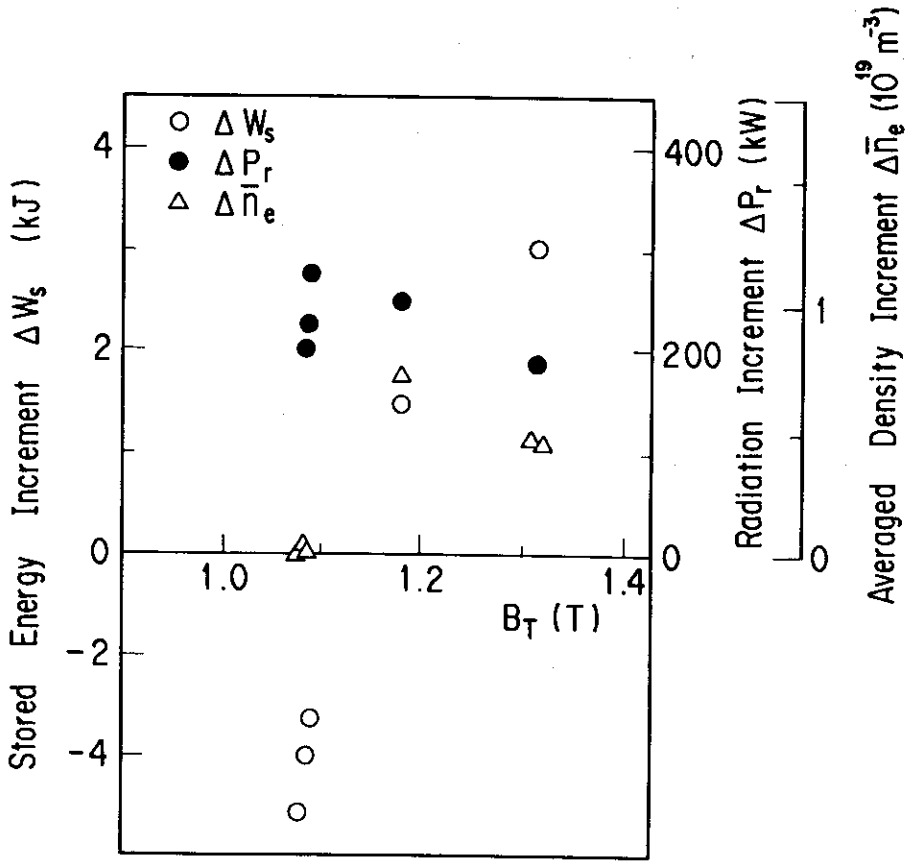

Fig.16 Increments dependence of stored energy(○), radiation loss(●), and density(△) on toroidal magnetic field strength during combination heating.

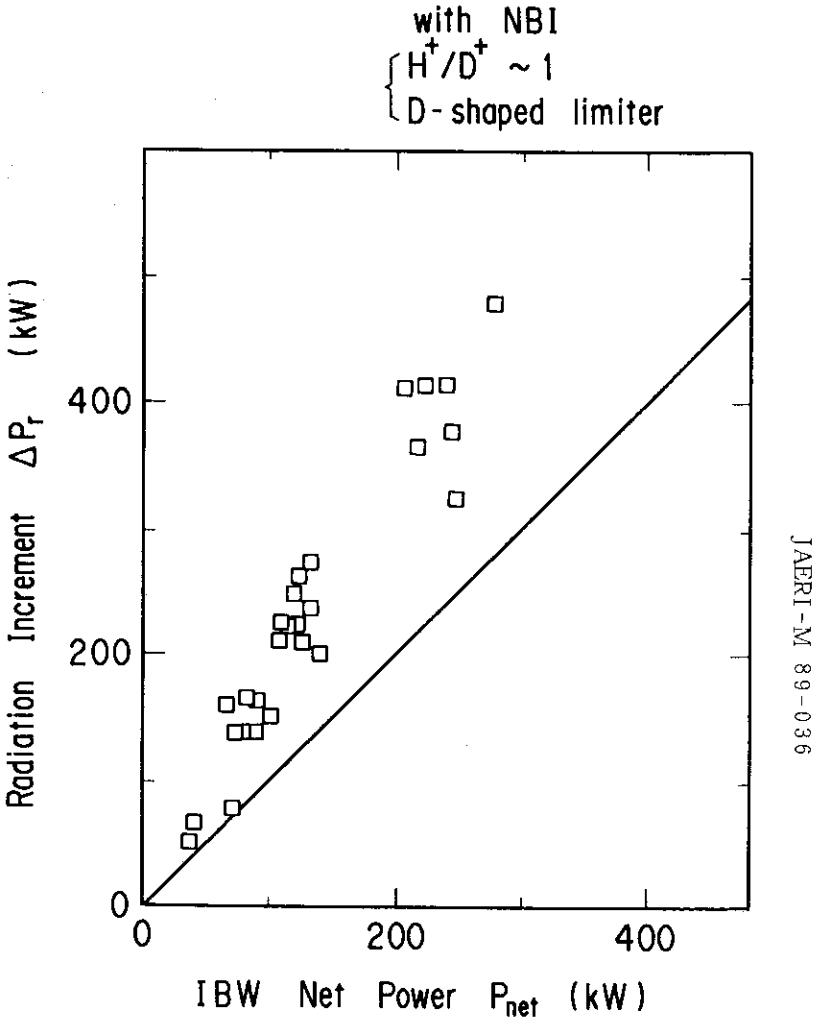

Fig.17 Increments of radiation during combination heating.

JAERI-M 89-036

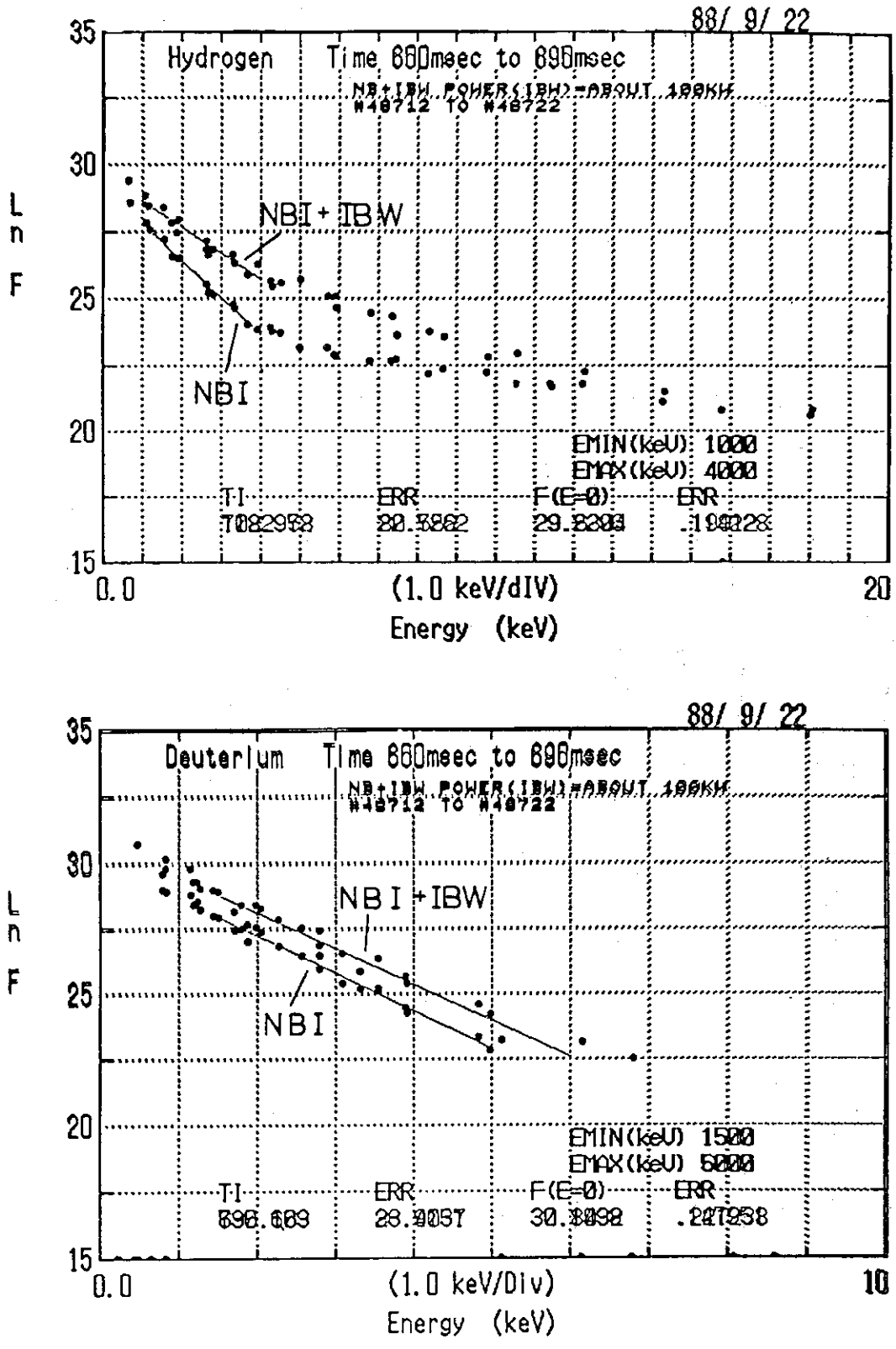

Fig.18 Energy spectrum of hydrogen and deuterium during combination heating.

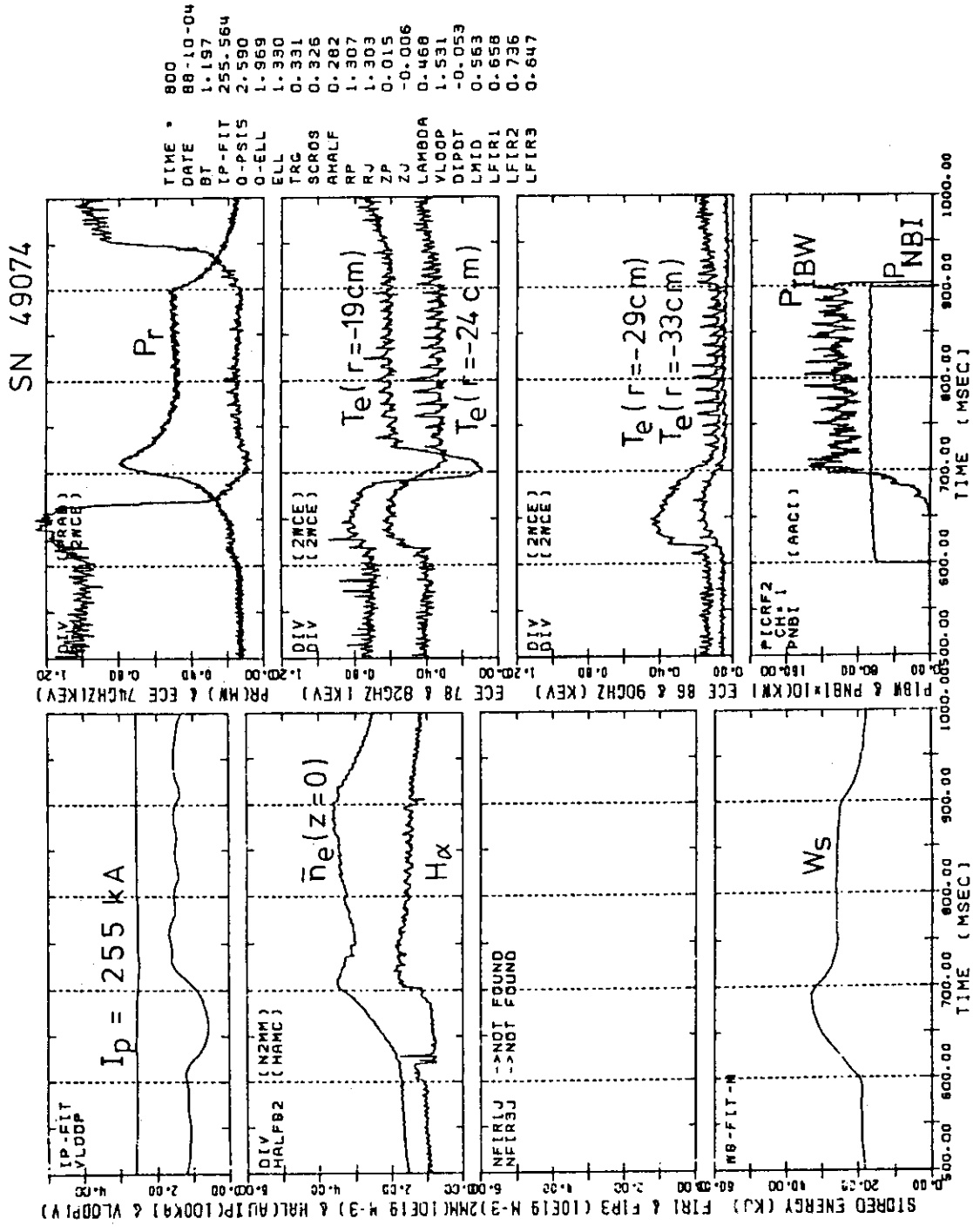

Fig.19 Temporal variation of typical plasma parameters with H-mode transition.

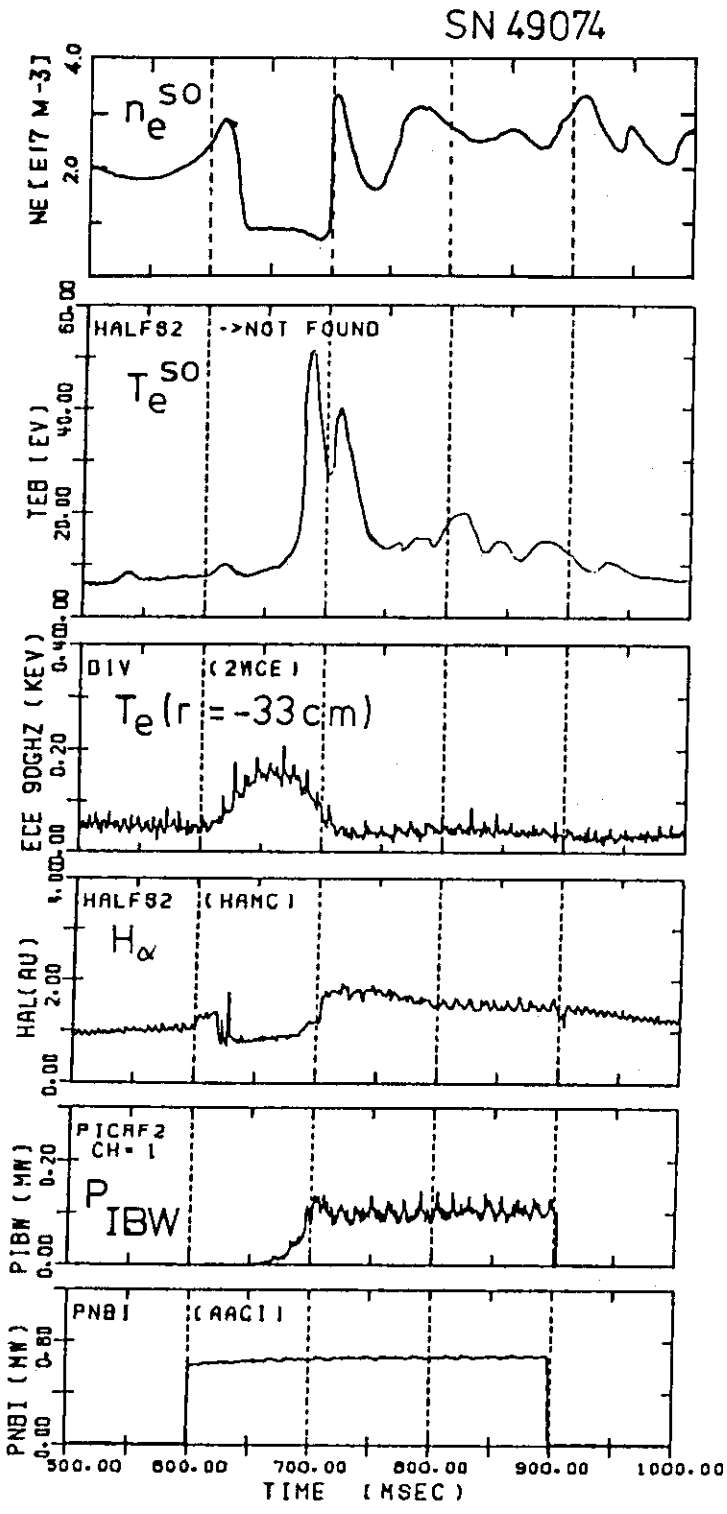

DT=	49074
TIME =	800
DATE	88-10-04
BT	1.197
IP-FIT	255.564
Q-PSIS	2.590
Q-ELL	1.969
ELL	1.330
TRG	0.331
SCROS	0.326
AHALF	0.282
RP	1.307
RJ	1.303
ZP	0.015
ZJ	-0.006
LAMBDA	0.468
VLOOP	1.531
DIPDT	-0.053
LMID	0.563
LFIR1	0.658
LFIR2	0.736
LFIR3	0.647

Fig.20 Temporal behavior of scrape-off electron temperature measured by electrostatic probe.

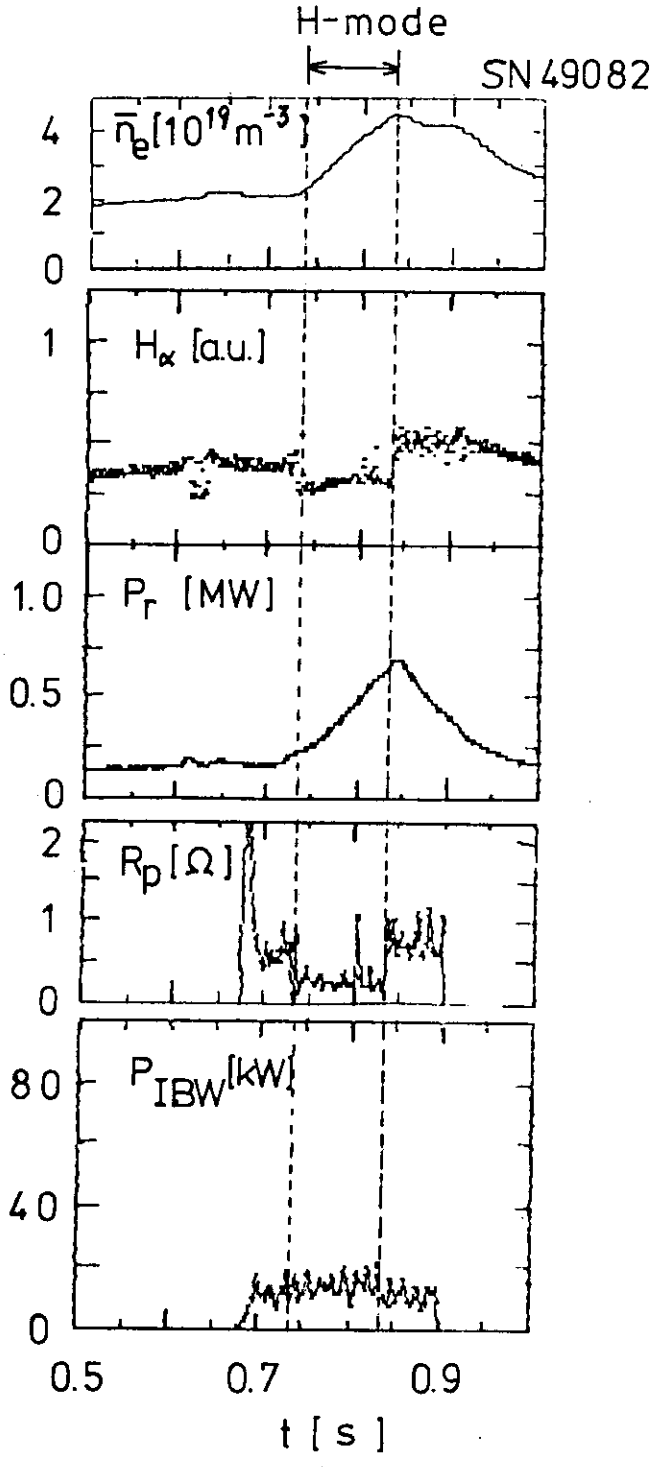

Fig.21 Loading impedance with H-mode plasma.